PHYSICAL REVIEW A VOLUME 23, NUMBER 3 MARCH 1981

Interaction of high-power laser pulses with atomic media. II. Optical second-harmonic generation

Kenzo Miyazaki, Takuzo Sato, and Hiroshi Kashiwagi

Laser Research Section, Radio- and Opto-Electronics Division, Electrotechnical Laboratory, 1-1-4 Umezono, Sakura-mura, Nihari-gun, Ibaraki 305, Japan

(Received 30 January 1980)

It is theoretically and experimentally demonstrated that optical second-harmonic generation (SHG) is possible to be observed in atomic media irradiated with an intense laser pulse. The SHG is induced by a static electric field spontaneously generated in the interaction, and any special condition is not required for the SHG. The experiment to observe the SHG has been made using atomic sodium vapor and a mode-locked Nd-doped yttrium aluminum garnet laser system (pulse duration, 28 psec; output energy $\lesssim 50$ mJ). The second harmonic (SH) polarization, spatial beam pattern, and dependences of SH signal on the sodium density and on the fundamental intensity have been examined. The experimental results agree well with the theoretical predictions and numerical results.

I. INTRODUCTION

In the preceding paper,[1] hereafter referred to as (I), it has been shown that an intense laser pulse irradiating an atomic medium inevitably induces static electromagnetic fields due to the laser radiation force in the medium. Optical second-harmonic (SH) radiation may be simultaneously generated in the atomic medium subjected to the laser beam.

In general, optical second-harmonic generation (SHG) or three-wave mixing in atomic vapors and gases is allowed under only certain restricted conditions, if high-order electric-quadrupole or magnetic-dipole moments are taken into account in atomic nonlinear susceptibilities.[2-6] In the electric dipole (El) approximation, SHG in centrosymmetric media is strictly forbidden by parity conservation or symmetry. However, the application of an external dc electric field to the medium removes this restriction, making it possible to observe SHG due to El interaction. This process is known as electric-field-induced SHG[7-10] and was demonstrated in atomic gases by several authors.[11,12] Mossberg *et al.*[5] have recently observed SHG in atomic thallium vapor without external field, and to explain the SHG, they proposed a radial electric field generation due to charge separation produced by ionization (with two-photon resonance) of atoms.

This paper presents an experiment and a theoretical analysis to show that SHG induced by spontaneously generated electric field is possible to be observed in an atomic vapor. The nonlinear optical process concerned is in principle the same as the electric-field-induced SHG mentioned above. However, in the present case, any external dc electric field or special conditions are not required for the SHG. The SH radiation is easily observed and may provide us with some information about the interaction of an intense laser pulse with atomic media. Some of the experimental results have been presented previously in a brief report.[13]

Section II gives a theory of the SHG induced by the spontaneous electric field in an atomic medium, where a short (~psec) laser pulse irradiating a dispersive atomic vapor is assumed. In Sec. III, we describe detail of the experiment in which use has been made of atomic sodium (Na) vapor and a mode-locked Nd-doped yttrium-aluminum-garnet (Nd : YAG) laser system. In Sec. IV, experimental and numerical results are presented and discussed. The discussion is concerned with the SH polarization and spatial beam pattern, characteristic natures of the generated SH pulse, and dependences of the SHG on Na density and fundamental intensity.

II. THEORETICAL

Let us consider an atomic vapor irradiated with a short (~psec) laser pulse. The conditions considered here are similar to those in (I) and are summarized as follows: The atomic vapor is isotropic and consists of one-electron atoms such as alkali-metal atoms; the incident laser beam, which is approximated by a plane wave, is linearly polarized and propagating along x and z directions, respectively, and has the intensity distribution I of the form $I = I_0 \psi(r) \phi(t)$, where ψ and ϕ are the dimensionless shape functions normalized with respect to the maximum field intensity I_0; the laser frequency ω is far from any kind of resonances of the atomic transitions. The irradiation of a laser pulse is accompanied with multiphoton ionization of atoms, which is inevitably apt to occur in the interaction of an intense laser pulse with atomic media. The other atomic or secondary processes, such as avalanche ioni-

zation, recombination, macroscopic current, and charge separation[5] between electron and ion distributions, in the ionized vapor are neglected because of the short interaction duration concerned. The field depletion due to multiphoton absorption for the ionization is so small that it may be ignored.

Under the conditions described above, as discussed in detail in (I), a static electric field $\langle \vec{E}_s \rangle$ due to laser radiation force is spontaneously generated in the medium. According to (I), the form for a component of $\langle \vec{E}_s \rangle$ is given, in the cylindrical coordinates, as

$$\langle E_s \rangle_r = \frac{2\pi e}{mc}\left((1-KF)\exp(-F)\sum_i \frac{f_i}{\omega_i^2-\omega^2} - [1-(1-KF)\exp(-F)]\frac{1}{\omega^2}\right)\frac{\partial I}{\partial r}, \quad (1a)$$

$$\langle E_s \rangle_\theta = 0, \quad \langle E_s \rangle_z \neq 0, \quad (1b)$$

where the dielectric constant $\epsilon(\omega)$ of the form

$$\epsilon(\omega) = 1 - \frac{4\pi e^2 N_e}{m\omega^2} + \frac{4\pi e^2 N}{m}\sum_i \frac{f_i}{\omega_i^2-\omega^2} \quad (2)$$

is employed for the atomic medium in which multiphoton ionization proceeds. In Eqs. (1) and (2), m, e, and c have the usual meanings, N and N_e are the densities of neutral atoms and ionization electrons, respectively, f_i is the oscillator strength for the transition i with excitation frequency ω_i, K is the minimum number of incident laser photons required to ionize a single atom, and using the multiphoton ionization probability W at the frequency ω for a specific kind of atoms, F is a quantity defined by

$$F = \int_{-\infty}^{t} W dt, \quad (3)$$

which is concerned with the degree of ionization of atoms at time t. Using the function F, the ionization rate N_e/N_0 is given by

$$N_e/N_0 = 1 - \exp(-F), \quad (4)$$

where $N_0 = N + N_e$ is the initial number density of neutral atoms.

Now, it can be easily shown that optical second-harmonic generation (SHG) is possible in the medium of interest. As is well-known, the SH radiation can be generated in the presence of an external *dc* electric field applied to atomic or centrosymmetric media.[7-12] Similarly, the spontaneous electric field $\langle \vec{E}_s \rangle$ may induce the SHG to be observed in atomic media, even if there are no external fields applied. The effective SH dipole moment $\vec{P}(2\omega)$ in this process[9,10] is associated with the static electric field $\langle \vec{E}_s \rangle$ and the incident high-frequency field $\vec{E}$ according to

$$\vec{P}(2\omega) = \chi^{(3)} \langle \vec{E}_s \rangle \vec{E}\vec{E}, \quad (5)$$

where $\chi^{(3)}$ is the effective third-order nonlinear susceptibility per unit volume of the medium. Equations (1) and (5) show that only the radial component of $\langle \vec{E}_s \rangle$ can contribute to the SH radiation to be observed in the z direction. Equation (5) is alternatively expressed by the components of $\vec{P}(2\omega)$ as

$$P_x(2\omega) = \chi_1^{(3)}(\langle E_s \rangle_r \cos\theta)E^2, \quad (6a)$$

$$P_y(2\omega) = \chi_2^{(3)}(\langle E_s \rangle_r \sin\theta)E^2, \quad (6b)$$

where the incident field $\vec{E}$ is polarized along the x direction, and θ is the angle between the fundamental polarization and $\langle E_s \rangle_r$. The susceptibility components may be written as $\chi_1^{(3)} = \chi_{xxxx}$ and $\chi_2^{(3)} = \chi_{yyxx} + \chi_{yxyx} + \chi_{yxxy}$. Equation (6) shows that the SH radiation predicted is linearly polarized, and that we have a radially polarized SH light along the x and y directions. For $\chi_1^{(3)} = \chi_2^{(3)}$, the SH radiation has a perfect radial polarization. Moreover, for an incident Gaussian beam, the SH light will vanish at the beam center ($r = 0$) on account of the form $\partial I/\partial r \propto rI$ for $\langle E_s \rangle_r$, which is given by Eq. (1), and of its radial polarization.

From Eq. (5), in the plane-wave approximation, the local and temporal SH intensity $I_{2\omega}$ generated along the z direction may be given by[9,10,14,15]

$$I_{2\omega} = C(\sin\tfrac{1}{2}\Delta kL/\tfrac{1}{2}\Delta kL)^2 \chi^2 N^2 \langle E_s \rangle_r^2 I^2, \quad (7)$$

where we have set $\chi^{(3)} = \chi N$ for the atomic vapor,[9,14] using the effective nonlinear susceptibility χ per atom, C is a constant, L is the interaction length, and Δk is the wave-vector mismatch between the fundamental and SH radiations. The wave-vector mismatch is given by $\Delta k = 4\pi(n_2 - n_1)/\lambda$, where n_1 and n_2 are the refractive indexes at the fundamental and SH wavelength λ and $\frac{1}{2}\lambda$, respectively, which can be easily derived from Eq. (2). The function $(\sin\frac{1}{2}\Delta kL/\frac{1}{2}\Delta kL)^2$ describes the phase-matching condition for the SHG, and the maximum conversion efficiency from ω to 2ω is attained with $\Delta k = 0$. In the present case of interest, Δk or the coherence length L_c defined by $L_c = |\pi/\Delta k|$ is a function of space and time since the ionization of atoms proceeds in the medium. If there is no ionization, the intensity $I_{2\omega}$ given by Eq. (7) has the fourth-power dependence of the fundamental intensity I because $\langle E_s \rangle_r$ is proportional to I.

Integration of Eq. (7) over the spatial coordinates gives the SH power $P_{2\omega}$, and the SH energy $E_{2\omega}$ is obtained from integrating $P_{2\omega}$ over the time t or the temporal history of the fundamental pulse. According to the principle described above, calculations of $I_{2\omega}$, $P_{2\omega}$, and $E_{2\omega}$ have been made on an incident Nd: YAG laser pulse irradiating atomic

Na vapor. The results will be discussed later together with the experimental results obtained.

III. EXPERIMENTAL

To demonstrate the SHG process predicted in Sec. II, an experiment was made using a mode-locked Nd:YAG laser system and atomic Na vapor. The laser system employed has been described in detail elsewhere,[16] and only the outline of the system will be repeated here. The oscillator was passively mode-locked by a saturable dye, and the TEM_{00}-mode laser beam from the oscillator was linearly polarized. A single pulse was selected from the mode-locked pulse train by an electro-optic shutter, spatially filtered, and amplified by three amplifiers up to the output energy of 50 mJ. The pulse duration τ of a single pulse was 28 psec, which was measured by the two-photon-fluorescence method, assuming a Gaussian temporal profile of the laser pulse. The spatial intensity distribution of the laser beam was measured with a photodiode array, and it was found to be in good agreement with a Gaussian profile. The beam divergence α was also estimated from the measurement of the spatial beam profile and was found to be $\alpha = 0.33$ mrad. Great care was taken to obtain a fine spatial quality of the beam in the operation of the laser system.

Figure 1 illustrates the experimental arrangement employed to observe the SHG. The atomic Na vapor is produced in a heat-pipe-type oven made of stainless steel, of which pressure is changed over the range from 0.1 to 1.0 Torr. Argon of about 3 Torr was used as the buffer gas. The oven is thermostatically controlled and provides a stable vapor zone of about 16 cm over the central region. The incident laser beam is focused by a lens with the focal length $L_f = 46$ cm into the oven containing the Na vapor. The spot size $r_0 = 152$ μm of the focused beam was determined from the relation $r_0 = \alpha L_f$.

The initial identification of the SH light generated in the Na vapor was made using a 100-cm spectrograph, on which the SH spectrum was observed together with a reference spectrum of helium. Photographic and photoelectric measurements of the SH radiation were carried out. In Fig. 1, the SH radiation generated in the oven is separated from the fundamental light by a dielectric mirror (M_1), while the fundamental energy of each laser shot is monitored by a calibrated pyroelectric energy meter (PE) and recorded on a storage oscilloscope (CRO I). The SH beam passes through an interference filter (IF) and is photographed by a Polaroid camera. The SH polarization is determined by observing the spatial beam pattern behind a polarizer (P_1). Also, the SH radiation is measured by a detection system composed of a 30-cm spectrometer and an optical multichannel analyzer (OMA). The SH signal $S_{2\omega}$ of the OMA is integrated during a laser pulse to give the relative SH energy. The SH signal detected is monitored on an oscilloscope (CRO II), and if necessary, it can be recorded on a X-Y recorder. Above the incident laser intensity of about 5×10^{11} W/cm^2, the SH radiation at $\lambda = 532$ nm could be easily observed both photographically and photoelectrically.

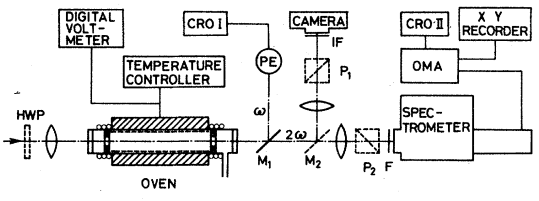

FIG. 1. Schematic diagram of the experimental arrangement. M_1, M_2, dielectric mirrors; P_1, P_2, polarizers; CRO I, CRO II, oscilloscopes; IF, interference filter; F, filter; OMA, optical multichannel analyzer; PE, pyroelectric energy meter; HWP, half-wave plate.

IV. RESULTS AND DISCUSSION

A. SH polarization and beam pattern

We now present the results obtained for the SHG in atomic Na vapor. As suggested in Sec. II, it should be the polarization and spatial beam pattern of the SH radiation that demonstrate the most distinctive properties of the SHG process predicted. In Fig. 2, we display the SH beam pattern observed. The upper one in Fig. 2 shows clearly

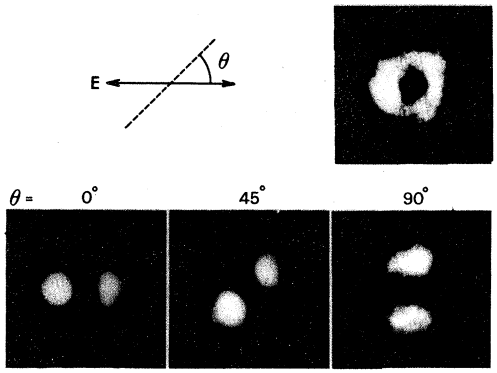

FIG. 2. Photographs of the SH beam pattern observed with no polarizer (the upper one) and behind a polarizer (the lower three). θ is the angle between the fundamental polarization and the polarizer axis, which are indicated by an arrow and a dashed line, respectively. Each photograph was taken by about 100 superimposed laser shots at the intensity $I_0 = (2 \sim 3) \times 10^{12}$ W/cm^2.

a ringlike pattern of the SH beam, that is, the SH is found to be never generated at the beam center ($r=0$). The lower three photographs in Fig. 2 indicate definitely that, for the incident linearly polarized Gaussian beam, the SH light is linearly polarized in the radial direction of the beam. The SH polarization determined is schematically shown in Fig. 3. We measured the SH signal $S_{2\omega}$ as a function of the angle θ between the fundamental and SH polarizations, and the result is shown in Fig. 4. No apparent dependence of $S_{2\omega}$ on θ has been found. This result is consistent with the radial polarization observed, implying that the nonlinear susceptibility $\chi^{(3)}$ defined in Eq. (5) is radially isotropic, or $\chi_1^{(3)} \approx \chi_2^{(3)}$ in Eq. (6), under the present experimental conditions. Thus the SH polarization and spatial beam pattern observed are in good agreement with the theoretical predictions described in Sec. II.

B. The SH pulse

Calculations of $I_{2\omega}$, $P_{2\omega}$, and $E_{2\omega}$ have been performed under nearly the same conditions as in the experiment. The method of calculations on the incident laser pulse and the spontaneous field is essentially the same as discussed extensively in (I). The incident Nd: YAG laser pulse is assumed to have Gaussian spatial and temporal intensity profiles of the form $I=I_0\exp(-2r^2/r_0^2)\exp(-4t^2/\tau^2)$ with the spot size $r_0=152$ μm and the pulse duration $\tau=28$ psec. In Eq. (7) providing the SH intensity $I_{2\omega}$, the nonlinear susceptibility χ is assumed constant, and the Na-vapor zone length L is taken to be 6.6 cm which is equal to the effective interaction length of multiphoton ionization[16] estimated for the present experimental condition of focusing.

Examples of the numerical results for $I_{2\omega}$ are represented in Fig. 5, which show the characteristic spatial profile of $I_{2\omega}$ in consistent with the ringlike beam pattern observed and displayed in Fig. 2. The temporal changes in the radial electric field $\langle E_s\rangle_r$ calculated under the same conditions as in Fig. 5 can be referred to in (I) (see also Appendix).

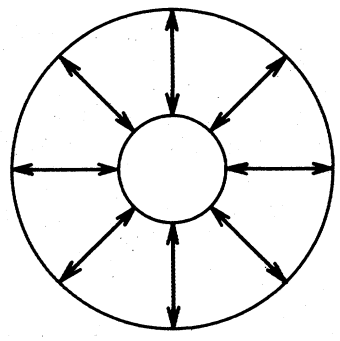

FIG. 3. Scheme of the SH polarization observed.

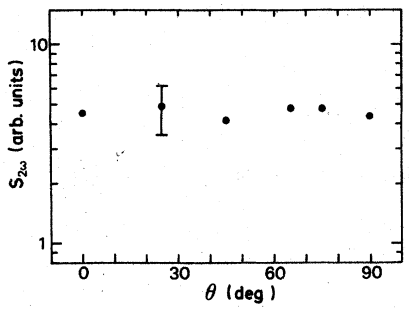

FIG. 4. SH signal observed as a function of the angle between fundamental and SH polarizations. Initial Na density $N_0=3.4\times10^{15}$ cm^{-3}; Fundamental intensity $I_0=3.0\times10^{12}$ W/cm^2.

Figure 6 shows the temporal changes in $P_{2\omega}$ at several fundamental intensities, which have been obtained by integrating $I_{2\omega}$ over the spatial coordinates, i.e., over r in this case. It is seen that the SH pulse is deformed from the incident Gaussian pulse due to the ionization and resulting temporal change in the phase mismatch Δk for the SHG. The calculated SH energy $E_{2\omega}$, which can be easily obtained by integrating $P_{2\omega}$ over the time t, will be compared with the experimental results in what follows.

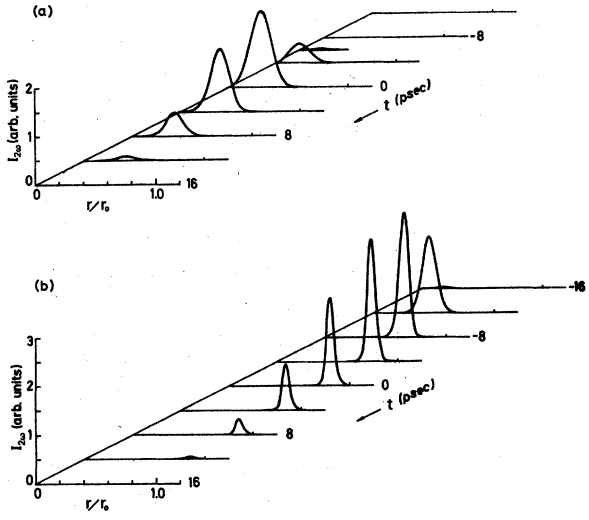

FIG. 5. Temporal changes in the radial distribution of SH intensity. The incident Nd: YAG laser pulse is assumed to have the duration $\tau=28$ psec and the spot size $r_0=152$ μm; Initial Na density $N_0=5.3\times10^{15}$ cm^{-3}; Interaction length $L=6.6$ cm; Fundamental intensity (a) $I_0=8\times10^{11}$ W/cm^2, (b) $I_0=3\times10^{12}$ W/cm^2.

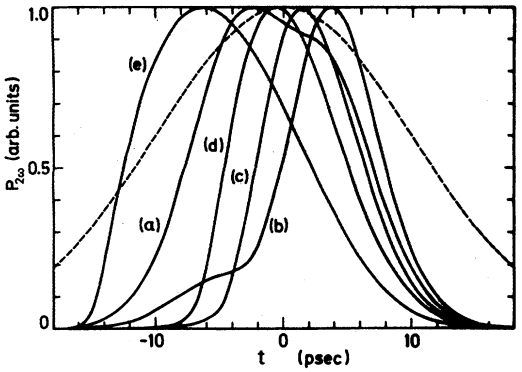

FIG. 6. Temporal dependences of SH power under the same conditions as in Fig. 5. Fundamental intensity I_0 = (a) 5×10^{11}, (b) 6×10^{11}, (c) 8×10^{11}, (d) 1×10^{12}, (e) 3×10^{12} W/cm^2. The dashed line indicates the temporal profile of the fundamental power.

C. Dependences of the SH energy on Na density and fundamental intensity

In Fig. 7, we show the numerical results for the SH energy $E_{2\omega}$ as a function of the initial Na density N_0 at the fundamental intensity I_0= (a) 5×10^{11}, (b) 8×10^{11}, and (c) 3×10^{12} W/cm^2, where the numerical conditions are the same as in Fig. 5. Note the large difference among the three dependences of $E_{2\omega}$ on N_0. At low input intensity, multiphoton ionization of Na atoms is so small that the wave-vector mismatch Δk does not change so much during the interaction. Then, as expected from Eq. (7), $E_{2\omega}$ has a periodic dependence [curve (a)] that is familiar to those obtained so far in the studies[15,17,18] of harmonic generation in atomic vapors. At high input intensity, a large change in Δk takes place in the interaction, because of the rapid and strong ionization of atoms. Then one can expect that the coherence length L_c becomes much longer than the initial value, and the phase-matching condition may be satisfied over the effective interaction region and duration for the SHG. For example, L_c is about 6 cm at $N_0=5\times10^{15}$ cm^{-3}, but when half of the neutral atoms are ionized, L_c becomes to be about 21 cm. Thus, $E_{2\omega}$ is nearly proportional to the square of N_0 at the high input intensity [curve (c)], as expected from Eq. (7).

To confirm the above prediction, the measurement of the SH signal $S_{2\omega}$ as a function of N_0 was made at a relatively high input intensity. The experimental result is shown in Fig. 8, where the calculated dependence and the slope of 2 are indicated by solid and dashed lines, respectively. The SH signal observed increases monotonously with increasing N_0 over the Na density region, as expected, being in excellent agreement with the calculated dependence.

We have also examined a dependence of the SHG on the fundamental intensity I_0, and the result is shown in Fig. 9. If the irradiation of a laser pulse

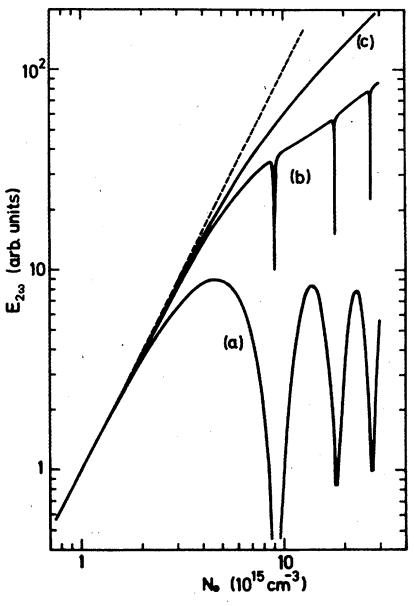

FIG. 7. Dependences of SH energy on initial Na density. Fundamental intensity I_0= (a) 5×10^{11}, (b) 8×10^{11}, (c) 3×10^{12} W/cm^2. The dashed line indicates a slope of 2. The numerical conditions are the same as in Fig. 5.

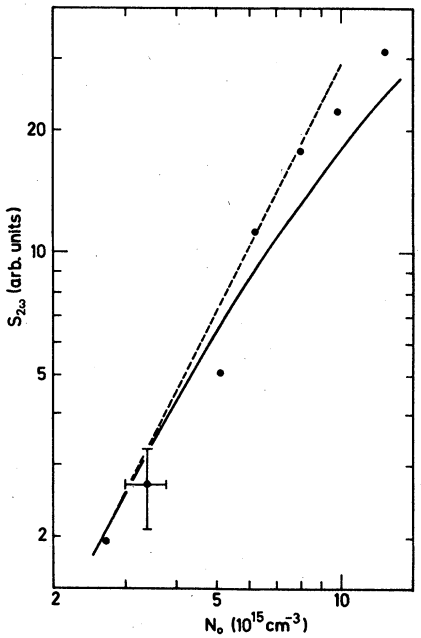

FIG. 8. SH signal observed as a function of the initial Na density. Fundamental intensity $I_0=2.8\times10^{12}$ W/cm^2. The calculated dependence of $E_{2\omega}$ on N_0 is shown by the solid line. The dashed line indicates a slope of 2.

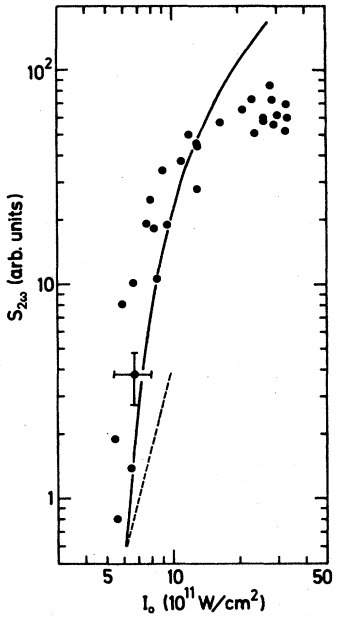

FIG. 9. SH signal observed as a function of the fundamental intensity. Initial Na density $N_0 = 5.3 \times 10^{15}$ cm^{-3}. The calculated dependence of $E_{2\omega}$ on I_0 is shown by the solid line. The dashed line indicates a slope of 4.

is not accompanied with the ionization of neutral atoms, the theory predicts a fourth-power dependence of $I_{2\omega}$ or $E_{2\omega}$ on I_0 (the dashed line in Fig. 9), as mentioned in Sec. II. However, the dependence observed shows a slope steeper than 4 at relatively low input intensities, and is reproduced well by the calculation in which the effects of ionization are incorporated (the dashed curve in Fig. 9). The saturation of $S_{2\omega}$ at high input intensities in Fig. 9 can be attributed to the rapid ionization of atoms in the interaction region.

V. CONCLUSION

The theory and experiment for the spontaneous-field-induced SHG have been presented. The experimental results for the SHG in atomic Na vapor irradiated with picosecond Nd:YAG laser pulses agree well with the theoretical predictions. The SHG is, in principle, possible whenever an intense laser pulse interacts with an atomic medium, and any special condition is not required for the SHG. From the observation of the SH radiation, especially, of the SH polarization and spatial beam pattern, one can see the static-field generation in the interaction of high-power laser pulses with atomic media.

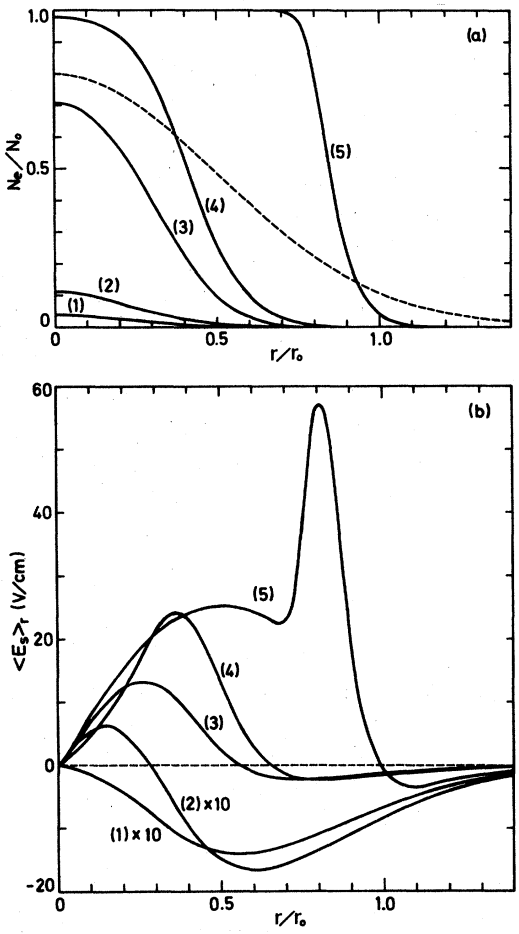

FIG. 10. Radial distribution of (a) multiphoton ionization rate and (b) radial electric field at the time $t = 0$. The numerical conditions are the same as in Fig. 5. Laser intensity I_0 = (1) 4×10^{11}, (2) 5×10^{11}, (3) 8×10^{11}, (4) 1×10^{12}, (5) 3×10^{12} W/cm^2. The dashed line indicated in (a) represents the intensity distribution of the incident laser beam.

ACKNOWLEDGMENTS

The authors wish to express their thanks to T. Honda, Dr. M. Yano, T. Kasai, F. Nemoto, and I. Matsushima for their helpful discussion and cooperation, and to Dr. K. Sakurai and Dr. K. Sugiura for their encouragement.

APPENDIX

Under the same conditions as in Fig. 5, we have calculated the multiphoton ionization rate N_e/N_0 and the radial electric field $\langle E_s \rangle_r$. Some examples of of the results have been shown in (I) and are reproduced in Fig. 10.

[1]K. Miyazaki, Phys. Rev. A 23, 1350 (1981).
[2]D. S. Bethune, R. W. Smith, and Y. R. Shen, Phys. Rev. Lett. 37, 431 (1976); Phys. Rev. A 17, 277 (1978).
[3]A. Flusberg, T. Mossberg, and S. R. Hartmann, Phys. Rev. Lett. 38, 59 (1977); 38, 694 (1977).
[4]M. Matsuoka, H. Nakatsuka, H. Uchiki, and M. Mitsunaga, Phys. Rev. Lett. 38, 894 (1977).
[5]T. Mossberg, A. Flusberg, and S. R. Hartmann, Opt. Commun. 25, 121 (1978).
[6]P. S. Pershan, Phys. Rev. 130, 919 (1963).
[7]R. W. Terhune, P. D. Maker, and C. M. Savage, Phys. Rev. Lett. 8, 404 (1962).
[8]P. D. Maker and R. W. Terhune, Phys. Rev. 137, A801 (1965).
[9]J. A. Armstrong, N. Bloembergen, J. Ducuing, and P. S. Pershan, Phys. Rev. 127, 1918 (1962).
[10]J. F. Ward, Rev. Mod. Phys. 37, 1 (1965).
[11]S. R. Finn and J. F. Ward, Phys. Rev. Lett. 26, 285 (1971).
[12]I. J. Bigio and J. F. Ward, Phys. Rev. A 9, 35 (1974).
[13]K. Miyazaki, T. Sato, and H. Kashiwagi, Phys. Rev. Lett. 43, 1154 (1979).
[14]J. F. Ward and G. H. C. New, Phys. Rev. 185, 57 (1969).
[15]R. B. Miles and S. E. Harris, IEEE J. Quantum Electron. QE-9, 470 (1973).
[16]K. Miyazaki and H. Kashiwagi, Phys. Rev. A 18, 635 (1978).
[17]J. F. Young, G. C. Bjorklund, A. H. Kung, R. B. Miles, and S. E. Harris, Phys. Rev. Lett. 27, 1551 (1971).
[18]H. Puell, K. Spanner, W. Falkenstein, W. Kaiser, and C. R. Vidal, Phys. Rev. A 14, 2240 (1976).

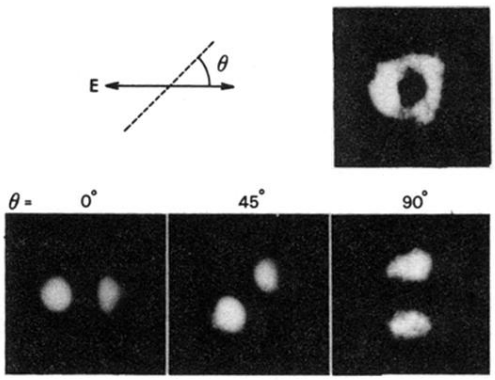

FIG. 2. Photographs of the SH beam pattern observed with no polarizer (the upper one) and behind a polarizer (the lower three). θ is the angle between the fundamental polarization and the polarizer axis, which are indicated by an arrow and a dashed line, respectively. Each photograph was taken by about 100 superimposed laser shots at the intensity $I_0 = (2 \sim 3) \times 10^{12}$ W/cm^2.